Eur. Phys. J. B **5**, 7–13 (1998)

THE EUROPEAN PHYSICAL JOURNAL B

Elasticity of BaFCl single crystal under hydrostatic pressure

F. Decremps[1,a], M. Fischer[1], A. Polian[1], and M. Sieskind[2]

[1] Physique des Milieux Condensés, Université Pierre et Marie Curie, B 77, 75252 Paris Cedex 05, France
[2] PHASE, 23 rue du loess, 67037 Strasbourg Cedex, France

Received: 19 March 1998 / Revised: 15 May 1998 / Accepted: 19 May 1998

Abstract. The sound velocities for longitudinal and transverse waves have been measured in single crystalline BaFCl at room temperature using ultrasonic pulse echo and Brillouin scattering techniques. The complete set of elastic constants is deduced and lead to the bulk moduli values of BaFCl at ambiant conditions ($B_0 = 44$ GPa, $B_\perp = 133$ GPa, $B_\parallel = 131$ GPa) which are compared with those obtained by a shell model. Moreover, using the ultrasonic technique under pressure, the pressure derivatives of the second order elastic constants at 298 K have been determined up to 0.3 GPa. All moduli increase linearly with pressure in this pressure range, allowing to determine directly and separately the first derivative of the bulk modulus $B'_0 = 5.8$. These data are used to calculate a Murnaghan equation of state. A detailed comparison is given between our results with those recently obtained by X-ray diffraction on powder or calculated using the local density approximation method. Finally, the anisotropy of BaFCl under pressure is discussed.

PACS. 62.20.Dc Elasticity, Elastic constants – 78.35.+c Brillouin scattering – 64.30.+t Equations of state of specific substances

1 Introduction

Layered compounds are characterized by their anisotropic bonding scheme. This anisotropy translates in several physical properties, particularly in the elastic properties and their pressure dependence. Barium fluorochloride BaFCl is a ionic compound which belongs to the layered crystal family of the natural mineral PbFCl, the matlockite. They are tetragonal crystals (P4nmm space group, [1]), characterized by six independent elastic constants: C_{11}, C_{33}, C_{44}, C_{66}, C_{12}, and C_{13}. BaFCl is formed by alternative sheets of BaF_2 and $BaCl_2$ (Fig. 1). The BaF_2 sub-lattice is formed by Ba_5 pyramids of cations linked by cations tetrahedra surrounding a fluor atom Ba_4F. The second sheet $BaCl_2$is made up of two types of polyhedra, one formed by a Ba_4 tetrahedron and the other one by a cation pyramid inside which the Cl anion is in an asymmetric coordination $Ba_{4+1}{-}Cl$ (which means that the distances between the anion and the cations are not isotropic: $Ba_4{-}Cl = 3.28$ Å and $Ba_1{-}Cl = 3.19$ Å). To shed some light on the elasticity of the matlockites, we report in this paper results at ambiant condition (obtained from Brillouin scattering and ultrasonics measurements), and, under hydrostatic pressure (from ultrasonics measurements, in the 0–300 MPa range) providing a basis for understanding the layered behaviour under pressure. The values of elastic moduli measured in isothermal and adiabatic conditions do not differ significantly for ionic solids, and, therefore, no difference will be made in this paper.

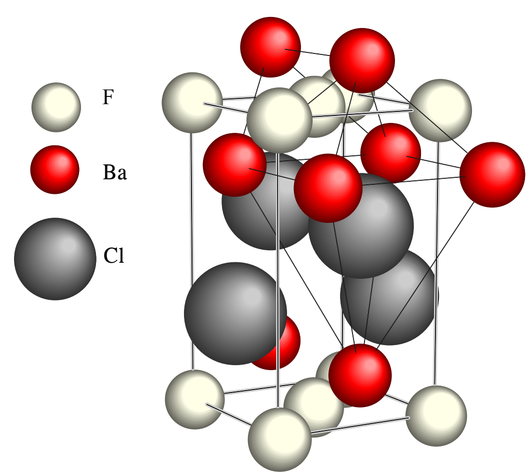

Fig. 1. BaFCl tetragonal structure.

[a] e-mail: fad@pmc.jussieu.fr

Table 1. Elastic moduli in tetragonal crystal related to ultrasonic wave velocity measurements for various propagation and polarization directions.

Propagation direction	Polarization direction	ρV^2	Mode
[100]	[100]	$C_{1}1$	pure (L_1)
[001]	[001]	$C_{3}3$	pure (L_2)
[100]	in (100) plan	$C_{6}6$	pure (T_1)
[001]	in (001) plan	$C_{4}4$	pure (T_2)
[110]	[1$\bar{1}$0]	$(C_{11}-C_{12})/2$	pure (T_3)
[110]	[110]	$(C_{11}+C_{12}+2\ C_{66})/2$	pure (L_3)
[10$\bar{1}$]	close to [10$\bar{1}$]	X_+	quasi (QL_1)
[10$\bar{1}$]	close to [101]	X_-	quasi (QT_1)

with $X_\pm = \frac{1}{4}(C_{11}+C_{33}) + \frac{1}{2}C_{44} \pm \frac{1}{4}\sqrt{(C_{11}-C_{33})^2 + 4(C_{13}+C_{44})^2}$

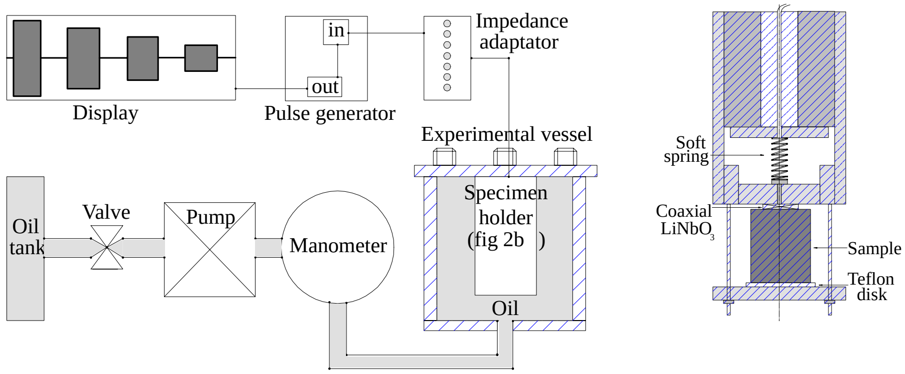

(a) (b)

Fig. 2. (a) Experimental set-up for ultrasonic measurements under hydrostatic pressure. (b) Sample holder.

2 Experimental procedure

2.1 Sample preparation

Single crystals were grown by slowly cooling a molten mixture of BaF_2 and $BaCl_2$ in a dry argon atmosphere. Details of the growth procedure have been published elsewhere [2]. The crystals were clear and colorless, with a typical dimensions of about $4 \times 5 \times 8$ mm^3, larger than the acoustical wavelength to insure that the sound pulse is transmitted as a plane wave. After one face of a crystal has been properly oriented (with an error less than 2 degrees), the opposite face of the sample is polished accurately parallel (within 1 degree) to the first one.

2.2 Ultrasonic measurements

The ultrasonic velocities and their stress derivatives were measured using a pulse echo overlap technique [3]. The output from an electrical wave source was used to apply pulses to the lithium niobate coaxial transducer (36 degree rotated Y-cut for longitudinal P-waves and 163 degree rotated X-cut for transverse S-waves). The transducers have been used at a frequency of 15 MHz for longitudinal waves (bonded to the specimen with an ultrasonic gel) and 18 MHz for transverse waves (bonded with Dow Resin 276 V9). Hydrostatic pressure up to 0.3 GPa was generated by a classical device including a manual pump, accurate manometers and a pressure cell having an internal volume of about 50 cm^3 (Fig. 2). The transmitting pressure medium was a Shell Tellus oil of low viscosity. The sample holder was especially built for brittle crystals such as the matlockite BaFCl (Fig. 2b).

At atmospheric pressure, the elastic moduli $\rho_0 V_0^2$ (ρ_0 is the density and V_0 the ultrasonic wave velocity at atmospheric pressure) were deduced from the acoustic pulse transit time and the path-length measurements. In order to determine the complete set of elastic moduli, four directions of ultrasonic wave propagation (in different polarization directions) are needed (Tab. 1).

Under pressure, the parameters actually measured are the natural wave velocities $W(P) = 2d_0/t(P)$ where d_0 is the unstressed path length and $t(P)$ the acoustic pulse transit time under pressure. If t_0 is the value of the transit time at atmospheric pressure, $W(P)$ is given by the following relation [4]:

$$W(P) = \frac{V_0}{1 + V_0\left(\frac{t(P)-t_0}{2d_0}\right)} \cdot \qquad (1)$$

Table 2. Brillouin scattering measurements of elastic moduli for various scattering configurations. X, Y, Z, T, U, V and W indicate the [100], [010], [001], [101], [10$\bar{1}$], [1$\bar{1}$0] and [110] directions, respectively. The configuration $A(B.)D$ indicates that the incident and scattered light are along the A and D directions, respectively, with the incident polarization vector parallel to B. The polarization of the scattered light is not analysed.

Configuration	ρV^2	Mode
$Y(X.)\overline{Y}$	C_{11}	pure L
$Z(V.)\overline{Z}$	C_{33}	pure L
$V(W.)\overline{W}$	$(C_{11}+C_{12}+2\ C_{66})/2$	pure T
$U(T.)\overline{U}$	Φ_+	quasi L
	Φ_-	quasi T
	Φ_T	pure T

with

$$\Phi_\pm = \frac{1}{2}\left(\Gamma_{11} + \Gamma_{33}\right) \pm \frac{1}{2}\sqrt{\left(\Gamma_{11} + \Gamma_{33}\right)^2 + 4\left(\Gamma_{13}\right)^2}$$

$$\Phi_T = \Gamma_{22}$$

where (θ is the angle between the phonon propagation direction and the [001] direction of the crystal):

$$\Gamma_{11} = C_{11}\sin^2\theta + C_{44}\cos^2\theta$$
$$\Gamma_{22} = C_{66}\sin^2\theta + C_{44}\cos^2\theta$$
$$\Gamma_{33} = C_{44}\sin^2\theta + C_{33}\cos^2\theta$$
$$\Gamma_{13} = (C_{13} + C_{44})\sin\theta\cos\theta$$

The pressure derivative of the elastic moduli ρV^2 corresponding to the direction of propagation n can be calculated from the pressure derivative of $\rho_0 W^2$. It can be shown that [5]:

$$\left(\frac{\delta(\rho V^2)}{\delta P}\right)_{P=0} = \left(\frac{\delta\left(\rho_0 W^2\right)}{\delta P}\right)_{P=0} - \rho_0 V_0^2\left[2\chi_n - \chi\right], \quad (2)$$

where χ is the isothermal bulk compressibility and χ_n the isothermal linear compressibility along the direction n.

2.3 Brillouin scattering measurements

The large parallelepipedic samples available for the ultrasonic experiments were also used to deduce the sound velocities in different directions of propagation (Tab. 2) from the measurement of the Brillouin shift $\Delta\sigma$ (in cm^{-1}) [6]:

$$V = \frac{\lambda_0 c \Delta\sigma}{2n\sin(\Phi/2)}, \quad (3)$$

where n is the refractive index at the wavelength of the laser light λ_0, c the velocity of light in vacuum, and Φ the angle between the incident and scattered photons. The average refractive index was measured by using an

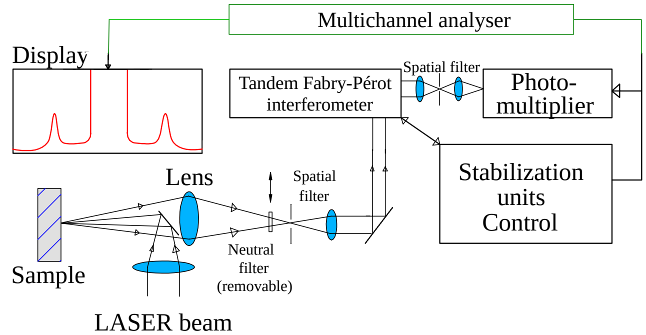

Fig. 3. Overall layout of the Brillouin-scattering spectrometer used in the present study.

Abbe refractometer. At the laser wavelength, its value is $n = 1.672(0.001)$. The main parts of the experimental setup are shown in Figure 3. The exciting light (the 514.5 nm of a single mode argon laser) is focused on the sample. The back-scattered light is collected by a lens,passes a spatial filter, the 6 pass tandem Fabry Pérot interferometer [7], a second spatial filter, and it is finally detected by a photomultiplier tube. In order to protect it from the high intensity of the unshifted Rayleigh line, a neutral density filter is interposed in front of the interferometer and it is synchronized with the piezoelectric scanning. Finally, the signal is processed by a photocounter and then stored in a multichannel analyser.

3 Results

3.1 Elastic constants at ambiant conditions

The elastic constants obtained from the two techniques are listed in Table 3. The agreement between the Brillouin scattering values and those obtained by ultrasonics is good considering the experimental uncertainties (which are related to the technique and also to the sample), and this conducted the choice of the selected value. The experimental values are compared with those calculated from a shell model [8]. The largest difference is for C_{66}, where the discrepancy is about 30%. From these values, the Debye temperature θ_D may be deduced using VRHG (Voigt-Reuss-Hill-Gilvarny) approximation [9]. It gives $\theta_D = 252.2$ K, in very good agreement with calorimetric measurements [10] $\theta_{calor} = 249$ K. This consistency between these results gives confidence in the specific-heat measurements and those of elastic constants which were made independently.

3.2 Pressure variation of the elastic constants

From the measurement of the pressure dependence of $\rho_0 W^2$ (see Fig. 4), the pressure derivative of the elastic moduli $\delta(\rho V^2)/\delta P$ is deduced using equation (2) and the appendix results. Using the effective elastic coefficients β_{IJ} which correspond to the effective elastic constants [11], the pressure derivative of β_{IJ} for the different

Table 3. Elastic constants of BaFCl. $\Delta C/C$ is equal to the difference between the calculated and the selected value divided by the selected one.

Elastic constant (GPa)	Ultrasonic value	Brillouin value	Selected value	Calculated value [8]	$\Delta C/C$ (%)
C_{11}	74.3 ± 0.8	74.3 ± 1.0	74.3 ± 0.8	90.8	22
C_{33}	65.7 ± 0.7	65.9 ± 0.8	65.8 ± 0.7	60.0	−10
C_{44}	21.0 ± 1	21.3 ± 0.8	21.1 ± 0.6	24.3	15
C_{13}	33.0 ± 2	36.0 ± 5	33.0 ± 2.0	41.6	26
C_{66}	24.1 ± 1.7	23.5 ± 1.1	23.8 ± 1.0	33.2	28
C_{12}	25.2 ± 2	24.9 ± 1.3	25.0 ± 1.4	26.7	6

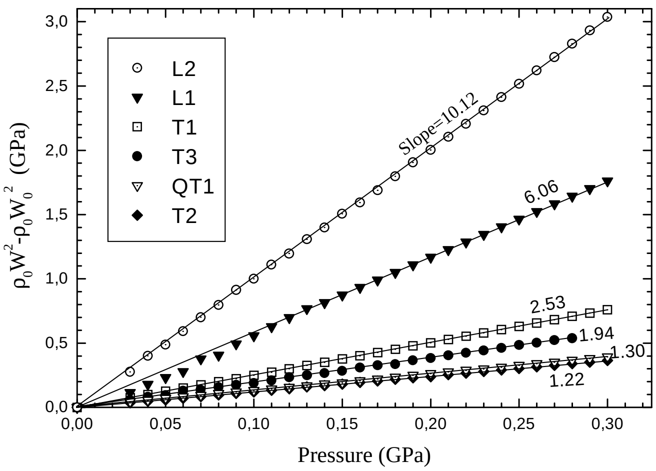

Fig. 4. Relative changes in natural velocity $W(P)$ induced by application of hydrostatic pressure. For each mode, the slope corresponding to the value of $\delta(\rho_0 W^2)/\delta P$ is given. The label of the modes fits the indications in equations (4) → (9) .

modes of propagation and polarization (see Tab. 1) are given by:
Longitudinal mode L_1:

$$\left(\frac{\delta\beta_{11}}{\delta P}\right)_{P=0} = \left(\frac{\delta\left(\rho_0 W^2\right)}{\delta P}\right)_{P=0} + C_{11}(0)\chi_{\parallel}. \quad (4)$$

Longitudinal mode L_2:

$$\left(\frac{\delta\beta_{33}}{\delta P}\right)_{P=0} = \left(\frac{\delta\left(\rho_0 W^2\right)}{\delta P}\right)_{P=0} - C_{33}(0)\left(\chi_{\parallel} - 2\chi_{\perp}\right). \quad (5)$$

Transverse mode T_1:

$$\left(\frac{\delta\beta_{66}}{\delta P}\right)_{P=0} = \left(\frac{\delta\left(\rho_0 W^2\right)}{\delta P}\right)_{P=0} + C_{66}(0)\chi_{\parallel}. \quad (6)$$

Transverse mode T_2:

$$\left(\frac{\delta\beta_{44}}{\delta P}\right)_{P=0} = \left(\frac{\delta\left(\rho_0 W^2\right)}{\delta P}\right)_{P=0} - C_{44}(0)\left(\chi_{\parallel} - 2\chi_{\perp}\right). \quad (7)$$

Transverse mode T_3:

$$\left(\frac{\delta\left(\frac{\beta_{11}-\beta_{12}}{2}\right)}{\delta P}\right)_{P=0} = \left(\frac{\delta\left(\rho_0 W^2\right)}{\delta P}\right)_{P=0} + \left(\frac{C_{11}(0) - C_{12}(0)}{2}\right)\chi_{\parallel}. \quad (8)$$

Quasi-transverse mode QT_1:

$$\left(\frac{\delta f(\beta_{IJ})}{\delta P}\right)_{P=0} = \left(\frac{\delta\left(\rho_0 W^2\right)}{\delta P}\right)_{P=0} + f\left(C_{IJ}(0)\right) + \chi_{\perp} \quad (9)$$

with

$$f\left(X_{IJ}\right) = \frac{1}{4}\left(X_{11} + X_{33}\right) + \frac{1}{2}X_{44} - \frac{1}{4}\sqrt{\left(X_{11} - X_{33}\right)^2 + 4\left(X_{13} - X_{44}\right)^2} \quad (10)$$

where $X_{IJ} = \beta_{IJ}$ or C_{IJ}. Then, from the knowledge of the pressure derivative of the effective coefficients $\beta'_{IJ} = \delta(\beta_{IJ})/\delta P$, the pressure derivative of the "thermodynamic" second order elastic constants $C'_{IJ} = \delta(C_{IJ})\delta P$ are calculated (see appendix). The complete results for the pressure-derivative coefficients are listed in Table 4. Again, the Debye temperature has been calculated within the VRHG approximation, which gives the pressure dependence of 9 K/GPa.

4 Analysis of results and discussion

4.1 Compressibilities at ambiant conditions

The linear compressibilities $\chi_{\parallel}$ ($\chi_{\perp}$) along a direction parallel (perpendicular) to the C_4 axis and the bulk compressibility χ are given by:

$$\chi_{\parallel} = \frac{\left(C_{11} + C_{12} - 2C_{13}\right)}{C_{33}\left(C_{11} + C_{12}\right) - 2C_{13}^2} \quad (11)$$

$$\chi_{\perp} = \frac{\left(C_{33} - C_{13}\right)}{C_{33}\left(C_{11} + C_{12}\right) - 2C_{13}^2} \quad (12)$$

and $$\chi = \chi_{\parallel} + 2\chi_{\perp}. \quad (13)$$

Table 4. Pressure derivative values of the effective (β_{IJ}) and thermodynamic (C_{IJ}) elastic constants at 298 K (dimensionless).

"*IJ*" coefficients	11	33	44	13	66	12
$\left(\frac{\delta\beta_{IJ}}{\delta P}\right)_{P=0}$	6.63 ± 0.05	10.60 ± 0.1	1.38 ± 0.02	5.92 ± 0.1	2.71 ± 0.03	2.13 ± 0.05
$\left(\frac{\delta C_{IJ}}{\delta P}\right)_{P=0}$	8.18 ± 0.06	12.13 ± 0.1	2.54 ± 0.02	5.17 ± 0.1	3.89 ± 0.05	1.31 ± 0.05

Table 5. Complete results on the BaFCl elastic properties.

Authors	Technique	$B_\perp$ (GPa)	$B_\parallel$ (GPa)	B (GPa)	B'
Shen *et al.* [16]	EDX	155 ± 10	237 ± 12	62 ± 6	4 ± 1
Beck *et al.* [14]	EDX	-	-	42 ± 10	4.5 ± 3
Balasubramanian *et al.* [8]	SM	105	195	41.4	-
Kalpana *et al.* [15]	TB	-	-	51.6	4
This work	US+BS	133 ± 13	131 ± 22	44.0 ± 5	5.8 ± 0.7

EDX: Energy dispersive X-ray diffraction experiments on powder with silicon-oil as pressure transmitting medium. US: Ultrasonics experiments. BS: Brillouin scattering experiments. SM: Shell Model calculations. TB: Calculations by the tight-binding linear muffin-tin orbital method within the local density approximation.

Their values are respectively (Tab. 5):

$$\chi_\parallel = (7.6 \pm 1.1) \times 10^{-3}\ \text{GPa}^{-1}$$
$$\chi_\perp = (7.5 \pm 0.7) \times 10^{-3}\ \text{GPa}^{-1}$$
$$\text{and} \quad \chi = (22.6 \pm 2.5) \times 10^{-3}\ \text{GPa}^{-1}.$$

The corresponding bulk and linear moduli are respectively:

$$B_0 = 44 \pm 5\ \text{GPa},$$
$$B_\parallel = 131 \pm 22\ \text{GPa}$$
$$\text{and} \quad B_\perp = 133 \pm 13\ \text{GPa}.$$

They are consistent with previous ultrasonic and Brillouin scattering measurements [13] and with the results of X ray diffraction obtained by Beck *et al.* [14]. Our results are also in good agreement with those given by the theory, either by a shell model calculation [8], or, more recently, by a local density approximation [15]. On the other hand, we note a large difference between our results and those obtained by Shen *et al.* [16] by energy dispersive X-rays diffraction, more particularly for the $B_\parallel$ values which differ by almost a factor of two (we find $B_\parallel = 131$ GPa instead of $B_\parallel = 237$ GPa given by Shen), hence the difference on B_0 is about 50%. This discrepancy may be due to the effect of non-hydrostatic conditions or grain-grain contact which may have affected the quality of the results, especially for $B_\parallel$ in a layered compounds like BaFCl. The comparison between the values of $\chi_\perp/\chi_\parallel$ in this crystal with those obtained in isostructural compounds MFX [13,17,18] gives the following results:

$$\left(\frac{\chi_\perp}{\chi_\parallel}\right)_{\text{BaFCl}} = 0.99 > \left(\frac{\chi_\perp}{\chi_\parallel}\right)_{\text{SrFCl}} = 0.95 >$$
$$\left(\frac{\chi_\perp}{\chi_\parallel}\right)_{\text{BaFBr}} = 0.76 > \left(\frac{\chi_\perp}{\chi_\parallel}\right)_{\text{SrFBr}} = 0.69 >$$
$$\left(\frac{\chi_\perp}{\chi_\parallel}\right)_{\text{BaFI}} = 0.4.$$

The difference of the $\chi_\perp/\chi_\parallel$ ratio between these compounds reveals the anisotropy of the bonding forces inside these crystals: the layers are principally bonded to each other by forces which weaken when an atom M or X is replaced by a larger one. Moreover, it appears that this effect is more pronounced when the halogen X is substituted for a larger one, which clearly lead to a layered structure as BaFI [19].

4.2 Compressibilities under pressure

The pressure derivative χ' of the bulk compressibility is related to the linear compressibilities and pressure derivatives of the effective elastic constants by [12]:

$$\chi' = -(2\chi_\perp Q_1 + \chi_\parallel Q_3)$$

with:

$$Q_1 = \chi_\perp [\delta(\beta_{11})/\delta P + \delta(\beta_{12})/\delta P] + \chi_\parallel \delta(\beta_{13})/\delta P$$
$$Q_2 = 2\chi_\perp \delta(\beta_{13})/\delta P + \chi_\parallel \delta(\beta_{33})/\delta P$$

The corresponding bulk modulus is deduced from the relation: $B_0' = -\chi'/\chi^2$

The values of these parameters are given in Table 5. These data are used to trace the Murnaghan equation of state [21] (see Fig. 5):

$$\frac{V}{V_0} = \left(1 + \frac{B_0'}{B_0} P\right)^{\frac{-1}{B_0'}}. \qquad (14)$$

The results as a whole are in good agreement with those obtained by theoretical calculations (using the local density approximation [15]). Obviously (see Sect. 4.1), there is a large difference between these results and the equation of state determined by Shen *et al.* [16]. Moreover, it should be noted that, contrary to what is obtained by the ultrasonics measurements, X-ray diffraction techniques do not allow to determine separately the couple (B_0, B_0'), leading to a significant uncertainty on each value.

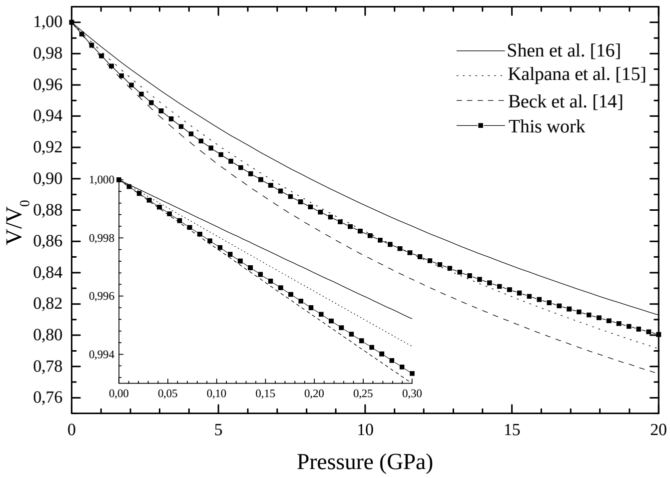

Fig. 5. Effect of pressure on the relative cell volume V/V_0 of BaFCl, for different values of B and B' from different authors, using the Murnaghan equation of state (around 21 GPa, a phase transformation occurs [16,22]).

5 Conclusion

The aim of this work was to determine the bulk moduli B_0, $B_{\|}$, $B_{\perp}$ and the pressure derivative of the bulk modulus B'_0 in single crystal BaFCl without any ambiguities due principally to the non-hydrostatic conditions inside the powder and the impossibility of knowing directly B'_0 in high pressure X-ray diffraction in a diamond anvil cell. The results are in good agreement with the theoretical values determined by local density approximation. Moreover, a previous study [19] on the behaviour of the BaFX elasticity under pressure showed that the X halogen anion plays an important role on the anisotropic character of these compound: the electronic polarizability of the X anion seems to be one of the most important causes of the observed structural anisotropy. These last assumptions give a good explanation for the pressure dependence of the BaFCl compressibilities, which are not (in the pressure range investigated) characteristic of a layered compound, according to the small polarizability of the chlorine (compared to those of bromine and iodine).

We would like to thank Mrs Lenain (Laboratoire d'Optique des Solides-UPMC) for her assistance in the index of refraction measurements and in the orientation and polishing of the crystals. Physique des Milieux Condensés is "unité mixte de recherche n° 7602" of the CNRS.

Appendix: Results in terms of pressure derivative of elastic moduli ρV^2 and linear/bulk moduli B for tetragonal structure (for more details, see [12] and [20])

Notations:

S_{IJ}: Compliance constant.
$\chi_{\perp}$ and $\chi_{\|}$: Linear compressibilities in the (100) plane and along the C_4 axis direction.
C_{IJ}: Isothermal thermodynamic elastic constant.
β_{IJ}: Isothermal effective elastic constant.
$\delta C_{IJ}/\delta P$: Pressure derivative of the thermodynamic elastic constant.
$\delta \beta_{IJ}/\delta P$: Pressure derivative of the effective elastic constant.
θ: Angle between the direction of propagation and the C_4 axis.

Pressure derivative of the effective elastic moduli ρV^2:

$$\left(\frac{\delta\left(\rho V^2\right)}{\delta P}\right)_{P=0} = \left(\frac{\delta\left(\rho_0 W^2\right)}{\delta P}\right)_{P=0} - \rho_0 V_0^2\left[2\chi_n - \chi\right] \quad \text{(A.1)}$$

with:

$$\chi_n = \chi_{\perp}\sin^2\theta + \chi_{\|}\cos^2\theta$$

and:

$$\begin{array}{ll} \chi_{\perp} = S_{11} + S_{12} + S_{13} & \chi_{\|} = 2S_{13} + S_{33} \\ S_{11} - S_{12} = 1/(C_{11} - C_{12}) & S_{33} = S(C_{11} + C_{12}) \\ S_{13} = -SC_{13} & S_{11} + S_{12} = SC_{33} \\ S = 1/[(C_{11} + C_{12})C_{33} - 2C_{13}^2] & 1/B = \chi = (2S_1 + S_3)/S^2. \end{array}$$

Effective (β_{IJ})-thermodynamic (C_{IJ}) coefficients:

$$\begin{array}{l} \delta(C_{11})/\delta P = \delta(\beta_{11})/\delta P + 1 - C_{11}(S_3 - 2S_1) \\ \delta(C_{13})/\delta P = \delta(\beta_{13})/\delta P - 1 + C_{13}S_3 \\ \delta(C_{12})/\delta P = \delta(\beta_{12})/\delta P - 1 - C_{12}(S_3 - 2S_1) \\ \delta(C_{33})/\delta P = \delta(\beta_{33})/\delta P + 1 - C_{33}(2S_1 - 3S_3) \\ \delta(C_{66})/\delta P = \delta(\beta_{66})/\delta P + 1 - C_{66}(S_3 - 2S_1) \\ \delta(C_{44})/\delta P = \delta(\beta_{44})/\delta P + 1 + C_{44}S_3. \end{array}$$

References

1. R.W. Wyckoff, *Crystal Structure*, (Interscience publishers, New York 1948).
2. M. Sieskind, M. Ayadi, G. Zachmann, Phys. Status Solidi b **136**, 489 (1986).
3. E.P. Papadakis, J. Acoust. Soc. Am. **42**, 1045 (1967).
4. H.J. McSkimin, P. Andreatch, J. Acoust. Soc. Am. **34**, 609 (1962).
5. D.C. Wallace, in *Solid State Physics*, **25**, edited by H. Ehrenreich, F. Seitz and D. Turnbull (Academic Press-New York and London, 1970), p. 301.
6. H.Z. Cummins, P.E. Schoen, in *Laser Handbook* edited by F.T. Arecchi and E.O. Schulz-Dubois, (North-Holland, Amsterdam, 1972) p. 1029.
7. J.R. Sandercock, in *Light scattering in Solids III*, edited by M. Cardona and G. Güntherodt, (Springer, Berlin, 1982) p. 173.

8. K.R. Balasubramanian, T.M. Haridasan, N. Krishnamurthy, Chem. Phys. Lett. **67**, 530 (1979).
9. S.W. Kieffer, Rev. Geophys. Space Phys. **17**, 1 (1979).
10. Y. Dossman, R. Kuentzler, M. Sieskind, D. Ayachour, Solid State Commun. **72**, 377 (1989).
11. β_{IJ}, the effective elastic constants, are the coefficients determined from Brillouin and ultrasonic experiments, commonly identified in the litterature as the elastic constants. However, it should be emphasized that those coefficients are different from the second derivatives of the internal energy with respect to the strain components when the strain is referred to the *unstressed* state, *i.e.* the "thermodynamic" elastic constants C_{IJ}. Actually, it is important to have in mind the physical process which occurs in a Brillouin or ultrasonic measurement: to probe the interaction potentials between the atoms, thermal excitations or ultrasonic waves are used, which involves additional deformations in the crystal (then, in a *stressed* state). The difference between β_{IJ} and C_{IJ} constants is therefore connected to the work function PV (when the crystal is under hydrostatic pressure) applied to the crystal by the external pressure.
    From a thermoelastic point of view [12], the effective elastic stiffness coefficients may be written in terms of the Gibbs free energy $G = F + PV$ (where F is defined as the free energy of the crystal) and of the components of the classical Lagrangian strain tensor $[\eta]$ as $\beta_{IJ} = [V^{-1}\delta^2 G/\delta\eta_I\delta\eta_J]$. On the other hand, the "thermodynamic" elastic constants, which correspond to the system under pressure without any additional deformation, is given by: $C_{IJ} = [V^{-1}\delta^2 F/\delta\eta_I\delta\eta_J]$. It follows that the propagation velocity of any mode under hydrostatic pressure can be obtained by replacing C_{IJ} by β_{IJ} in the appropriate zero-pressure formula. Although $\beta_{IJ} = C_{IJ}$ as the pressure is neglected(with respect to the value of the elastic coefficients), the pressure derivatives of the two set of quantities are different.
12. D.C. Wallace, *Thermodynamics of Crystals*, (Wiley, New York, 1972).
13. M. Fischer, M. Sieskind, A. Polian, A. Lahmar, J. Phys. Condens. Matter **5**, 2749 (1993).
14. H.P. Beck, A. Limmer, W. denner, H. Schulz, Acta. Cryst. B **39**, 401 (1983).
15. G. Kalpana, B. Palanivel, I.B. Shameem Banu, Phys. Rev. B **56**, 3532 (1997).
16. Y.R. Shen, U. Englisch, L. Chudinovskikh, F. Porsch, R. Haberkorn, H.P. Beck, W.B Holzapfel, J. Phys. Condens. Matter **6**, 3197 (1994).
17. F. Decremps, M. Fischer, A. Polian, M. Sieskind, High Temp. High Press. **30**, (to be published).
18. M. Fischer, A. Polian, M. Sieskind, J. Phys. Condens. Matter **6**, 10407 (1994).
19. F. Decremps, M. Fischer, A. Polian, M. Sieskind, The Review of High Pressure Science and Technology **7**, (to be published).
20. R.N. Thurston, J. Acoust. Soc. Am. **41**, 1093 (1966).
21. F. Birch, J. Geophys. Res. **57**, 227 (1952).
22. F. Decremps, M. Fischer, A. Polian, J.P. Itié, (unpublished).